Pharm Res (2013) 30:2868–2879
DOI 10.1007/s11095-013-1116-2

RESEARCH PAPER

Altered Brain Uptake of Therapeutics in a Triple Transgenic Mouse Model of Alzheimer's Disease

Dharmini C. Mehta • Jennifer L. Short • Joseph A. Nicolazzo

Received: 3 February 2013 / Accepted: 4 June 2013 / Published online: 22 June 2013

ABSTRACT

Purpose The purpose of this study was to systematically assess the impact of Alzheimer's disease (AD)-associated blood–brain barrier (BBB) alterations on the uptake of therapeutics into the brain.

Methods The brain uptake of probe compounds was measured in 18–20 month old wild type (WT) and triple transgenic (3×TG) AD mice using an *in situ* transcardiac perfusion technique. These results were mechanistically correlated with immunohistochemical and molecular studies.

Results The brain uptake of the paracellular marker, [^{14}C] sucrose, did not differ between WT and 3×TG mice. The brain uptake of passively diffusing markers, [^{3}H] diazepam and [^{3}H] propranolol, decreased 54–60% in 3×TG mice, consistent with a 33.5% increase in the thickness of the cerebrovascular basement membrane in 3×TG mice. Despite a 42.4% reduction in P-gp expression in isolated brain microvessels from a subpopulation of 3×TG mice (relative to WT mice), the brain uptake of P-gp substrates ([^{3}H] digoxin, [^{3}H] loperamide and [^{3}H] verapamil) was not different between genotypes, likely due to a compensatory thickening in the cerebrovascular basement membrane counteracting any reduced efflux of these lipophilic substrates.

Conclusion These studies systematically assessed the impact of AD on BBB drug transport in a relevant animal model, and have demonstrated a reduction in the brain uptake of passively-absorbed molecules in this mouse model of AD.

D. C. Mehta • J. A. Nicolazzo (✉)
Drug Delivery, Disposition and Dynamics
Monash Institute of Pharmaceutical Sciences, Monash University
381 Royal Parade, Parkville, Victoria 3052, Australia
e-mail: joseph.nicolazzo@monash.edu

J. L. Short
Drug Discovery Biology, Monash Institute of Pharmaceutical Sciences
Monash University, Parkville, Victoria 3052, Australia

KEY WORDS Alzheimer's disease · blood–brain barrier · cerebrovascular basement membrane · *in situ* transcardiac perfusion · P-glycoprotein · triple transgenic

ABBREVIATIONS

3×TG	triple transgenic
AD	Alzheimer's disease
APP	amyloid precursor protein
Aβ	amyloid-β
BBB	blood–brain barrier
CNS	central nervous system
CSF	cerebrospinal fluid
GFAP	glial fibrillary acidic protein
KBR	krebs carbonate-buffered physiologic saline
MVB	microvessel buffer
PBS	phosphate buffered saline
PFA-PBS	paraformaldehyde phosphate buffered saline
P-gp	P-glycoprotein
PS1	presenilin 1
WT	wild type

INTRODUCTION

Alzheimer's disease (AD) is characterized by two significant neuropathological alterations (described by Alois Alzheimer in 1907); namely senile plaques and neurofibrillary tangles consisting of amyloid-β (Aβ) deposits and hyperphosphorylated tau proteins, respectively (1). While there is currently no cure for AD, there exist treatments which improve the mental health of AD patients by retarding symptomatic progression. These Food and Drug Administration (FDA) approved treatments include three cholinesterase inhibitors (galantamine, rivastigmine and donepezil) and the N-methyl-D-aspartate receptor antagonist memantine (2). In order for any of these drugs to reach their site of action within the central nervous

system (CNS), they must cross the blood–brain barrier (BBB) following systemic administration. Under healthy conditions, the BBB is a diffusion barrier that maintains the homeostasis of the neuronal environment by regulating the free exchange of solutes between the blood and the brain, and by protecting the brain from xenobiotics, including drugs (3). However BBB dysfunction has been demonstrated in AD in various studies and is emerging as a vital pathological trait (4,5).

BBB-related pathological changes reported in AD include altered expression of transport proteins including P-glycoprotein (P-gp), low density lipoprotein receptor-related protein 1 and the glucose transporter (GLUT-1), disruption to inter-endothelial tight junction proteins, reduced cerebral perfusion, thickening of the capillary basement membrane, altered endothelial cell metabolic activity and altered capillary density (5–9). While there has been much research into the identification of these BBB alterations during AD, less is known about what impact such changes have on the ability of therapeutic agents to traverse the BBB, and whether such alterations could indeed lead to increased or decreased access of drugs into the brain. The notion that BBB drug transport in AD patients could differ from healthy individuals is rapidly attracting attention and very recently has been highlighted by various researchers (4,10,11). Due to their age, AD patients are simultaneously taking many other commonly prescribed medications and if there is increased BBB transport of systemically acting drugs into brain, this could lead to potential neurotoxicity. In contrast, decreased transport of AD drugs into the brain could plausibly lead to inefficient treatment and further symptom progression in AD. Therefore, a better understanding of the impact of AD on the BBB transport of therapeutic agents is required.

Suggestions of increased CNS access of blood-borne agents (and therefore BBB hyperpermeability) in AD stemmed from early studies demonstrating an increased concentration of plasma albumin and/or other immunoglobulins in the cerebrospinal fluid (CSF) of AD patients relative to healthy subjects (12). However, in contrast to the above findings, there have also been studies depicting no change in CSF levels of albumin in AD patients (13). Regardless, the above studies are more likely to be reflective of potential changes occurring at the blood–CSF barrier, rather than at the BBB. To further investigate potential changes to BBB permeability in AD, *in vivo* studies depicting the presence or absence of high molecular weight endogenous or exogenous protein markers (albumin and immunoglobulin G) in brain parenchyma have been undertaken in AD animal models, where again conflicting results have been reported (14–16). The studies to date assessing BBB permeability in AD have mainly focussed on the appearance of large molecular weight endogenous agents within the CNS, with less known about the disposition of smaller drug-like molecules in this disease. The few studies that have assessed the impact of AD on the BBB transport of small drug-like molecules (diazepam, clioquinol, PBT 2 and GSK-A and GSK-B) depicted limited change to the brain exposure of these drugs in AD mouse models (17–20). However, the brain uptake of each of these above-listed compounds was assessed in different animal models of AD, using different techniques for assessing brain uptake. To date, there has been no systematic comparative study assessing the BBB transport of a series of drug-like molecules (with varying mechanisms of transport across the BBB) in one single mouse model of AD. Such a study would provide invaluable insight into whether the CNS access of therapeutic agents is indeed altered in AD.

The purpose of this study, therefore, was to systematically assess the CNS disposition of various small-molecular weight compounds with varying mechanisms of BBB transport in a relevant AD mouse model. The compounds were chosen as markers of paracellular diffusion, passive transcellular diffusion and P-gp efflux (Table I) (21–24). The triple transgenic (3×TG) AD mouse model was selected for these studies as it exhibits age-related AD pathology similar to that observed in human AD patients (25) and all transport studies were carried out at 18–20 months of age, an age reported to resemble a severe form of AD (26). The BBB permeability of drugs can be measured using a number of *in vivo* techniques such as internal carotid artery injection, *in situ* carotid artery perfusion, intravenous bolus injection, brain efflux index and intracerebral microdialysis (27). Compared to other *in vivo* techniques, the *in situ* transcardiac perfusion technique provides a more accurate and sensitive method to determine BBB transport of molecules without confounding blood/plasma associated factors, such as alterations to plasma protein binding and/or systemic metabolism that may be observed in a disease phenotype (23). For these reasons, a transcardiac perfusion mouse model was employed to assess the brain uptake of probe compounds, a technique which has been used by other laboratories to assess the transport of large molecular weight compounds and proteins (28). Following the systematic evaluation of BBB transport in the 3×TG AD mice, various molecular studies (isolation of cerebral microvessels and quantification of P-gp levels and cerebrovascular membrane thickness) were undertaken to

Table I Probe Compounds and Their Mechanism of Transport Across the BBB

Probe compound	Mechanism of BBB transport
[^{14}C] sucrose	Paracellular diffusion
[^{3}H] diazepam	Passive transcellular diffusion
[^{3}H] propranolol	Passive transcellular diffusion
[^{3}H] digoxin	Active P-gp efflux
[^{3}H] verapamil	Active P-gp efflux
[^{3}H] loperamide	Active P-gp efflux

clarify potential mechanisms responsible for the altered brain uptake observed in our *in vivo* studies.

MATERIALS AND METHODS

Materials

[^{3}H] diazepam, [^{3}H] digoxin, [^{3}H] loperamide, [^{3}H] propranolol, [^{3}H] verapamil, Ultima Gold™ scintillation fluid, and Solvable™ were purchased from Perkin Elmer Life Sciences (Boston, MA). [^{14}C] sucrose was purchased from American Radiolabeled Chemicals, Inc. (St. Louis, MO). C219 antibody against P-gp was obtained from Signet Laboratories (Dedham, MA). Anti-β actin and anti-collagen-IV antibodies were purchased from Abcam (Cambridge, MA), and mouse β-tubulin III (TUJ1) was obtained from Covance Inc. (North Ryde, New South Wales, Australia). Goat anti-mouse IRDye® 680 antibody was purchased from LI-COR Biosciences (Lincoln, NE), and mouse anti-glial fibrillary acidic protein (GFAP), rabbit anti-mouse (Alexa Flour® 488) and donkey anti-mouse (Alexa Fluor® 532) antibodies were purchased from Life Technologies™ (Mulgrave, Victoria, Australia). Anti-von Willebrand factor (VIII) antibody, goat serum, dextran (70 kDa) and all other chemicals and reagents were purchased from Sigma-Aldrich (Castle Hill, New South Wales, Australia). Water was obtained from a Milli-Q water purification system (Millipore, Bedford, MA).

Animal Model of AD

3×TG AD mice harboring three mutant genes: beta-amyloid precursor protein (APP_{swe}), presenilin-1 ($PS-1_{M146V}$) and tau_{P301L} and the corresponding wild-type (WT) mice were provided by Prof Frank LaFerla (University of California, Irvine) and bred at the Monash Animal Research Platform, Australia. Tail DNA samples from WT and 3×TG mice were routinely genotyped to confirm the absence or presence of APP, PS1 and tau transgenes in WT and 3×TG mice, respectively. All animal experiments were approved by the Monash Institute of Pharmaceutical Sciences Animal Ethics Committee and performed in accordance with the National Health and Medical Research Council guidelines for the care and use of animals for scientific purposes.

In Situ Transcardiac Perfusion

This technique is widely used for assessing the brain disposition of large molecular weight compounds and has been validated in our laboratory and previously used by our group (28,29). WT and 3×TG mice (n=6 mice/probe compound, at 18–20 months of age) were anaesthetized with an intraperitoneal injection of ketamine (133 mg/kg) and xylazine (10 mg/kg). Once anaesthetized, the jugular veins were localized and marked with thread (silk braided, non-absorbable surgical suture). The thorax was opened and the heart exposed. The descending artery was localized and marked with thread directly behind the heart. Before starting the perfusion through the left ventricle, the jugular veins were cut and the descending artery clamped. The perfusion was performed at a rate of 2 mL/min. Each radiolabelled probe compound (0.5 μCi/mL) was prepared in Krebs carbonate-buffered physiologic saline (KBR) containing 128 mM NaCl, 24 mM $NaHCO_3$, 4.2 mM KCl, 2.4 mM NaH_2PO_4, 1.5 mM $CaCl_2$, 0.9 mM $MgCl_2$, and 9 mM D-glucose. The solution was gassed with 95% O_2/5% CO_2 for pH control (7.4) and warmed to 37°C prior to commencing the perfusion. Following a 4 min perfusion, the mice were killed by cervical dislocation and the whole brain was removed. The brain was carefully dissected to obtain the cortex and hippocampus, given that these are the main regions of the brain affected in AD (30), and these brain regions were placed into pre-weighed tubes. Cortical and hippocampal samples were digested overnight in 2 mL of Solvable™ at 50°C and neutralized with 30% v/v hydrogen peroxide before mixing with 10 mL of Ultima Gold™ scintillation cocktail. Aliquots (10 μL) of the perfusate were also collected to determine tracer concentrations in the perfusate (measured following the addition of 2 mL of Ultima Gold™ scintillation cocktail and vortex-mixing). [^{3}H] or [^{14}C] radioactivity was then determined using a Perkin Elmer 2800TR liquid scintillation analyzer (Boston, MA).

Calculations of Brain-to-Perfusate Ratio

All calculations were carried out as described previously in the literature (23). In brief, the apparent tissue distribution volume of the probe compounds (V_{brain}, mL/g) was calculated using Eq. (1):

$$V_{brain} = {}^{X_{brain}}\!/_{C_{perf}}, \text{ also referred as brain} - \text{to} - \text{perfusate ratio} \quad (1)$$

where X_{brain} is the concentration of probe compound detected in the cortical or hippocampal homogenate (ng/g) and C_{perf} is the concentration of probe compound in the perfusate (ng/mL). The total drug mass in the cortical or hippocampal homogenate was corrected for the amount of drug remaining in the brain microvasculature by Eq. (2):

$$X_{brain} = X_{tot} - V_{vasc} \times C_{perf} \quad (2)$$

where X_{tot} is the total quantity of probe compound in the cortical or hippocampal homogenate (parenchyma and

cerebrovasculature) (ng/g) and V_{vasc} is the cerebral microvascular plasma volume, which was determined by Eq. (3):

$$V_{vasc} = {X^*_{brain}}\Big/{C^*_{perf}} \quad (3)$$

where X^*_{brain} is the concentration of [^{14}C] sucrose in the cortical or hippocampal homogenate (ng/g) and C^*_{perf} is the concentration of [^{14}C] sucrose in the perfusate (ng/mL) following perfusion of [^{14}C] sucrose. The V_{vasc} determined in both WT and 3×TG mice was used for all subsequent corrections in the relevant genotype.

Collagen-IV Immunohistochemistry

Membrane thickness is one of the factors affecting the permeability of molecules diffusing across a biological membrane and given reports of a thickening of the cerebrovascular basement membrane in AD (7,31), cerebrovascular basement membrane thickness was measured in the AD mouse model used in our study. The apparent thickness of the vascular basement membrane was assessed immunohistochemically by measuring collagen-IV deposition in WT and 3×TG mice, as collagen-IV is one of the inherent components of the basement membrane (6). WT and 3×TG AD mice (n=3 per group) were transcardially perfused at a rate of 2 mL/min with 0.5% *v/v* heparinised saline and then 4% *w/v* paraformaldehyde in phosphate buffered saline pH 7.4 (PFA-PBS). Brains were removed and immersed in a cryopreservative–fixative solution (30% *w/v* sucrose in PFA-PBS) overnight at 4°C and stored at −80°C until sectioning. Brains were then implanted in Tissue Tek® O.C.T. (Sakura Finetek, Torrance, CA), cut into 30-μm coronal sections with a cryostat, thaw-mounted onto SuperFrost Plus® slides (Menzel-Glaser, Braunschweig, Germany), desiccated at room temperature and stored at −80°C until probed with antibodies.

Immunostaining of collagen-IV on brain slices was carried as per Bourasset *et al.* with minor modifications (17). Briefly, brain slices were washed in 0.1 M PBS and blocked with 10% *v/v* normal goat serum in 0.1 M PBS containing 0.2% *v/v* Triton-X 100 and the slices were then incubated in a humidified chamber for 1 h. After washing three times with 0.1 M PBS, sections were incubated with anti-mouse collagen-IV (1:500) in 0.1 M PBS containing 1% *v/v* normal goat serum and 0.2% *v/v* Triton X-100 at 4°C overnight. After incubation with the primary antibody, sections were washed three times with 0.1 M PBS and incubated with donkey anti-rabbit Alexa Fluor® 488 secondary antibody (1:1000) in 0.1 M PBS for 1 h at room temperature. After a further five washes in 0.1 M PBS (5 min each), sections were mounted with Vectashield mounting media (Vector Laboratories, Burlingame, CA), coverslipped, sealed and dried for 1–2 h at room temperature. Immunostaining for collagen-IV was examined under an Olympus BX61 fluorescence microscope attached to a CCD camera (DP30BW) (Olympus Corporation, Tokyo, Japan).

The cerebrovascular basement membrane thickness (as indicated by collagen-IV deposition) and the diameter of collagen positive stained microvessels were measured on digital pictures using Image J software (NIH, http://rsb.info.nih.gov/ij/). A total of eight images per animal were taken at 60× magnification and were evenly distributed between the primary motor cortex and parieto-temporal cortex (with four different brain sections for each cortical region). The images were first calibrated in Image J software against the scale obtained from the fluorescence microscope. The basement membrane thickness (collagen deposition) and diameter of 15 microvessels per animal/genotype were then measured (in μm) on blinded images using the tool "Analyze" available in Image J software.

Isolation and Characterization of Mouse Brain Capillaries

In order to correlate the brain uptake of P-gp substrates with the expression of cerebral microvascular P-gp, brain microvessels were isolated from WT and 3×TG mice and P-gp expression determined in these isolated microvessels by Western blot. Microvessels were isolated as previously described by Yousif *et al.* (32), with a few modifications, and all steps were conducted at 4°C. Briefly, Swiss Outbred mice (n=7–8 mice) or WT and 3×TG mice (n=7–8 mice/isolation, n=3 isolation/genotype) were anesthetized by isoflurane inhalation and decapitated. Groups of WT and 3×Tg AD mice (n=7–8 mice/isolation) were referred to as "sub-populations" of mice from each genotype. Swiss Outbred mice were used in the development and validation processes for isolating mouse brain capillaries. Brains were immediately removed and placed in ice cold microvessel buffer (MVB) (15 mM HEPES, 147 mM NaCl, 4 mM KCl, 3 mM $CaCl_2$, 1.2 mM $MgCl_2$, 5 mM glucose, and 0.5% *w/v* bovine serum albumin (BSA), pH 7.4). Cortical shells were separated from the cerebellum, meninges, brain stem and large superficial blood vessels and homogenized in MVB with a dounce homogenizer (Tissue Grinder, Potter-ELV) with 20 up-and-down manual strokes. The resulting homogenate was centrifuged at 1,000×g for 10 min. The pellet obtained at this step was suspended in 17% *w/v* dextran (70 kDa) and centrifuged for 90 min at 3,901×g. The supernatant containing the myelin layer was carefully removed and the resulting pellet was suspended in MVB. The obtained crude vessel suspension was then passed through a 100-μm mesh nylon filter (BD Biosciences, North Ryde, New South Wales, Australia) to remove cell debris and larger vessels. The filtrate obtained was then passed through a 20-μm mesh nylon filter (Merck, Victoria, Australia) and the fraction retained was washed with MVB

without BSA and centrifuged at 1,000×g for 40 min. The resulting capillaries were suspended in MVB and stored at −80°C if not immediately required for further processing. Freshly isolated brain microvessels were transferred onto glass slides (coated with rat tail collagen), incubated at 37°C for 1.5 h and fixed for 15 min with 4% PFA at room temperature. After washing with PBS, microvessels were permeabilised for 30 min with 0.5% (*v*/*v*) Triton X-100 in PBS and subsequently blocked with 1% *w*/*v* BSA in PBS. Microvessels were incubated overnight at 4°C with the primary antibody to either P-gp (1:50), von Willebrand factor VIII (1:800), β-tubulin (1:800) or GFAP (1:1000). If the microvessels were pure, they should show positive staining for P-gp and von Willebrand factor VIII, and negative staining for β-tubulin and GFAP. After washing with PBS, microvessels were incubated for 1 h at room temperature with the corresponding anti-mouse Alexa Fluor® 532 or anti-rabbit Alexa Fluor® 488-secondary antibodies (1:1000). After further washes in PBS, microvessels were mounted with Vectashield mounting media (Vector laboratories, Burlingame, CA) and visualized using fluorescence microscopy.

Western Blot for P-gp

Isolated mouse brain capillaries were lysed for 45 min at 4°C in lysis buffer containing 150 mM NaCl, 50 mM Tris–HCl pH 7.4, 0.5% *v*/*v* Triton X-100, 0.5% *w*/*v* sodium deoxycholate and the protease inhibitor cocktail Complete (Roche Diagnostics, Castle Hill, New South Wales, Australia). The lysates were centrifuged at 15,000×g for 15 min and the supernatant containing membrane proteins was stored at −80°C until further use. The total protein concentration was determined with a Pierce® BCA protein assay (Thermo Scientific, Rockford, IL) using BSA as a standard. Protein samples were prepared in Laemmli buffer by heating at 70°C for 10 min. A mass of 3.5 μg of total protein was loaded onto 8% *w*/*v* polyacrylamide gels and resolved at 125 V by SDS gel electrophoresis (Mini-protean Tetra System, Bio-Rad Laboratories, Gladesville, New South Wales, Australia). Resolved proteins on the gel were electroblotted onto a nitrocellulose membrane (0.2 μm, Protran™, GE Healthcare, Rydalmere, New South Wales, Australia) for 2 h using a semi-dry transfer cell (Trans-blot® SD, Bio-Rad Laboratories, Gladesville, New South Wales, Australia). Non-specific binding sites were blocked with 5% (*w*/*v*) non-fat dried milk in TBS-T buffer containing 10 mM Tris–HCl pH 7.5, 200 mM NaCl and 0.1% (*v*/*v*) Tween 20. Membranes were then incubated overnight at 4°C with mouse monoclonal C219 P-gp (1:100) and mouse β-actin (1:1000) antibody in TBS-T buffer containing 1% (*w*/*v*) non-fat dried milk. After washing with TBS-T buffer, membranes were incubated in goat anti-mouse IRDye® 680 secondary antibody (1:15000) for 2 h at room temperature and washed with TBS-T buffer before the P-gp and β-actin protein bands were visualized using the Odyssey® Infrared Imaging system (LI-COR Biosciences, Lincoln, NE).

Statistical Analysis

All data are presented as mean ± standard error of the mean (SEM) unless otherwise stated. For comparison of brain-to-perfusate concentration ratios or comparison of basement membrane thickness, microvessel diameter and P-gp expression between WT and 3×TG mice, Student's unpaired t tests were applied using SPSS for Windows (SPSS statistics 19, IBM) with a p value < 0.05 considered significant.

RESULTS

Determination of BBB Paracellular Integrity

Following transcardiac perfusion of [^{14}C] sucrose, no significant difference was observed in the hippocampus to perfusate (H:P) or cortex to perfusate (C:P) ratio between WT and 3×TG mice. The H:P and C:P ratios of [^{14}C] sucrose in WT and 3×TG mice (Fig. 1) were in agreement with the normal distribution volume of [^{14}C] sucrose in mouse brain reported in ours and other laboratories (29,33).

Brain Uptake of Passively Diffusing Transcellular Markers

In contrast to our observations for paracellular transport, we observed altered brain uptake of transcellular passive markers in 3×Tg AD mice. A substantial and significant reduction of 57% and 54% in the hippocampal and cortical

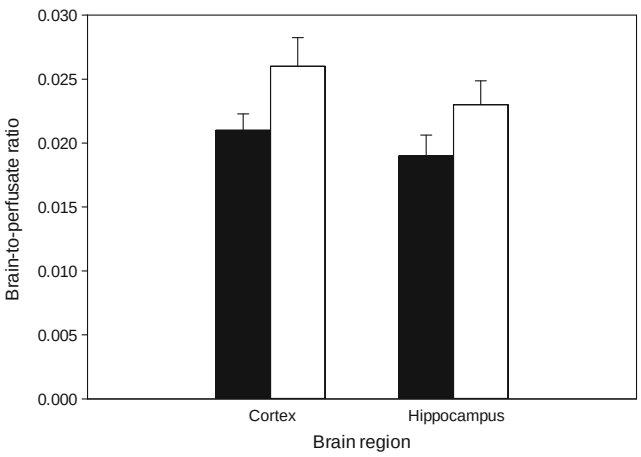

Fig. 1 Brain-to-perfusate ratio of [^{14}C] sucrose in cortex and hippocampus following transcardiac perfusion of WT (■) and 3×TG (□) mice. Data are presented as mean ± SEM ($n = 6$–7 mice).

uptake, respectively, of [^{3}H] diazepam was observed in 3×TG mice (relative to WT mice) (Fig. 2a). Similarly, a 47% reduction in the hippocampal uptake of [^{3}H] propranolol and a significant 62% reduction in the cortical uptake of [^{3}H] propranolol was observed in 3×TG mice, relative to WT mice (Fig. 2b).

Measurement of Cerebrovascular Basement Membrane Thickness

To determine whether the reduction in [^{3}H] diazepam and [^{3}H] propranolol brain uptake in AD mice may have been due to cerebrovascular basement membrane thickening (and therefore, reduced passive diffusion), the thickness of the vascular basement membrane was assessed immunohistochemically by measuring collagen-IV deposition. As shown qualitatively (Fig. 3a–d), the cerebral microvessels in 3×TG mice appeared to exhibit more intense collagen-IV staining and were more irregular in shape relative to the microvessels in WT mice. When quantifying the deposition of collagen IV using Image J, there was a 33.5±5.5% increase in collagen-IV deposition in 3×TG mice, concordant with an increased thickness of the cerebrovascular basement membrane (Fig. 3g) and an increased path length necessary for the passively-diffusing molecules to enter the brain parenchyma. Furthermore, there was no difference in the measured internal diameter of the microvessels between WT and 3×TG mice (Fig. 3h).

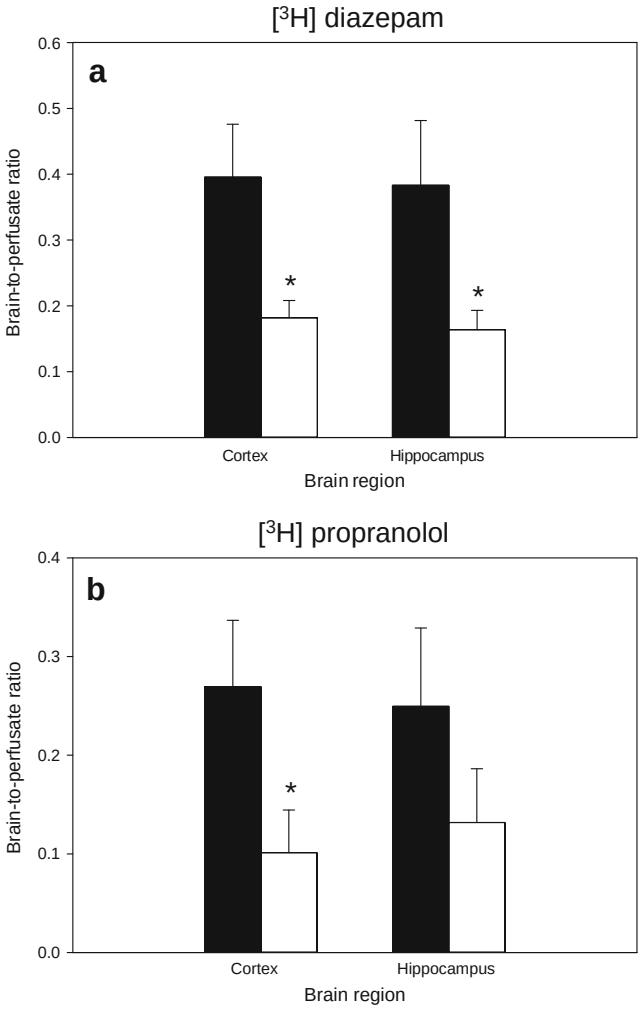

Fig. 2 Brain-to-perfusate ratio of transcellular passive markers (**a**) [^{3}H] diazepam and (**b**) [^{3}H] propranolol in cortex and hippocampus following transcardiac perfusion of WT (■) and 3×TG (□) mice. Data are presented as mean ± SEM (n = 6–7 mice). * Indicates a significantly (P < 0.05) lower brain-to-perfusate ratio in 3xTG AD mice relative to WT mice using an independent samples t-test.

Brain Uptake of P-gp Substrates

To determine the impact of potential changes of P-gp expression in AD, the brain uptake of well-known P-gp substrates was evaluated in WT and 3×TG mice. Though [^{3}H] digoxin showed an increasing trend in its brain uptake in 3×TG mice in comparison to WT mice, the increment was not substantial enough to be significant (Fig. 4a). Furthermore when P-gp functional activity was measured with two other well-known P-gp substrates, a similar observation was noted. There was no significant difference in the cortical or hippocampal uptake of [^{3}H] loperamide and [^{3}H] verapamil between WT and 3×TG mice (Fig. 4b,c).

Expression of P-gp in Isolated Cerebral Microvessels

Given that there was no difference in the brain uptake of P-gp substrates in 3×TG mice, it was essential to investigate whether P-gp expression was indeed reduced in this mouse model of AD. We firstly validated the brain microvessel isolation procedure by characterizing the molecular expression profile of cerebral microvessels isolated from Swiss Outbred mice (6–8 weeks of age). The isolated microvessels were pure without any gross contamination from neuronal or glial cells as seen in phase contrast images of isolated microvessels (Fig. 5a). Upon immunostaining of these isolated microvessels, positive expression of von Willebrand factor, a marker for all endothelial cells, and P-gp, a specific marker for BBB endothelial cells, was observed, while there was no staining for neuronal and glial cell markers, confirming the lack of neuronal cells and astrocytes (Fig. 5b–d). Once we had characterized the isolated microvessels from Swiss Outbred mice, microvessels were isolated from a group of WT and 3×TG mice (n=7–8 mice for each genotype) followed by Western blotting for P-gp. P-gp expression was reduced by 42.4±0.7% (n=3) in 3×TG mice relative to WT mice (Fig. 6a). Although we had confirmed reduced expression of P-gp in this set of 7–8 mice (one sub-population), we repeated the determination of P-gp expression from two more sub-populations of 3×TG and WT mice (n=7–8 mice for each sub-population/genotype). Here we observed a 17% decrease in 3×TG mice from one group

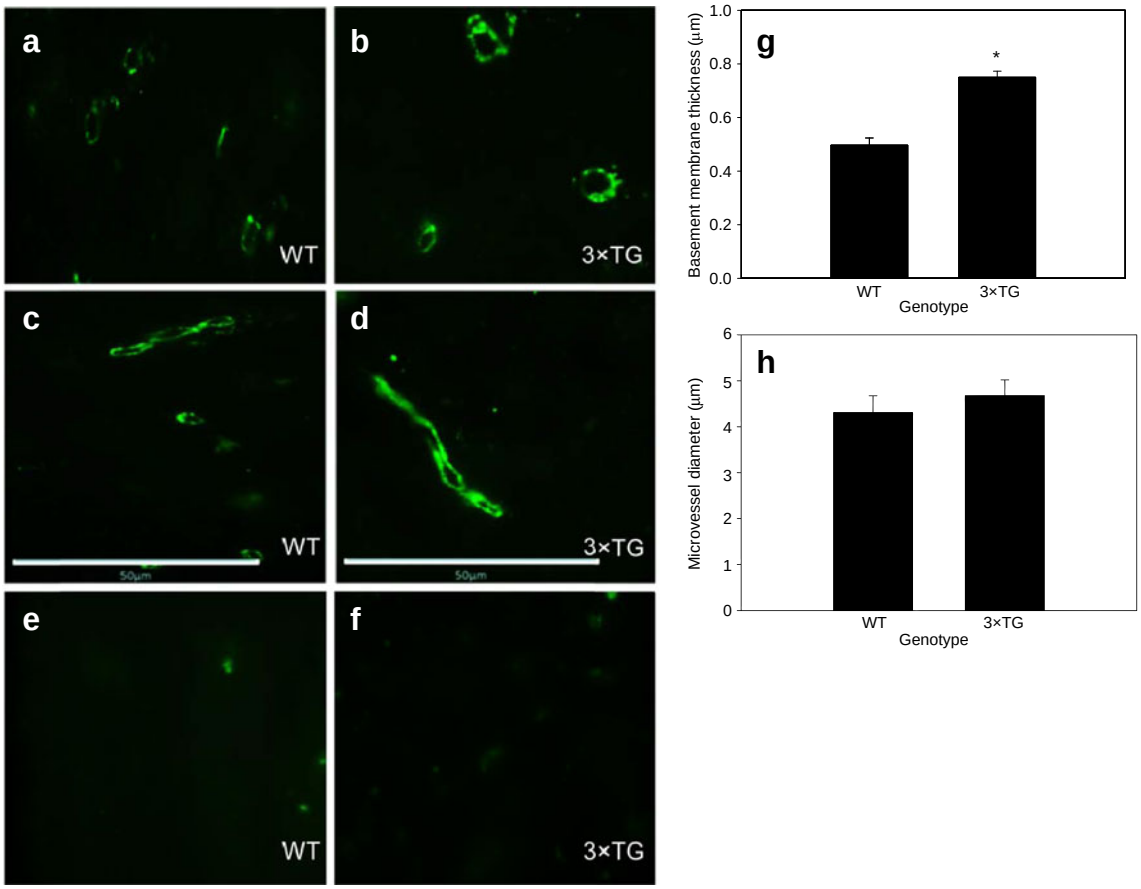

Fig. 3 Cerebrovascular basement membrane thickening depicted by collagen-IV deposition in cortical brain sections of WT and 3×TG mice. Microvessels from the cerebral cortex of 3×TG mice (**b** and **d**) displayed more intense immunolabeling of collagen-IV when compared to WT mice (**a** and **c**). Note that collagen-IV staining is absent in negative control brain sections from WT and 3×TG mice where no primary antibody was included (**e** and **f**). The basement membrane thickness is significantly ($p < 0.05$) increased in microvessels from 3×TG mice (**g**) with no significant difference in the capillary diameter detected between WT and 3×TG mice (**h**). Data are represented as mean ± SEM of 3 mice per genotype. * Indicates a significant ($p < 0.05$) increase in the basement membrane thickness in 3×TG mice relative to WT mice, using an independent samples *t*-test.

while no reduction in P-gp expression was observed in 3×TG mice from a third sub-population (Fig. 6b,c). Thus it was observed that the expression of P-gp was significantly reduced in 3×TG mice relative to WT mice, though there was variability in its expression amongst the different populations of 3×TG mice.

DISCUSSION

AD is associated with multiple pathophysiological and neurochemical changes that lead to functional alterations and physical changes in the BBB (5). As drug disposition to the CNS is primarily limited by the function of the BBB, any changes to this barrier will potentially affect the CNS disposition of systemically-administered drugs. Given that the status of the BBB in AD appears controversial (4), and there is even less known about how this impacts on CNS exposure of drugs, this study assessed the brain uptake of various probe molecules in the 3×TG AD mouse model. Radiolabelled probe compounds were selected based on their mechanism of transport across the BBB. [^{14}C] sucrose was chosen as a marker of paracellular transport (23), with the hypothesis that if the inter-endothelial tight junctions are indeed disturbed then there will be increased brain uptake of [^{14}C] sucrose, a compound whose entry is normally restricted in the vascular space. [^{3}H] diazepam and [^{3}H] propranolol exhibit high brain uptake and passively diffuse across the BBB under healthy conditions (21,24), and are therefore suited as relevant markers to determine disease-related changes in the BBB transcellular pathway. [^{3}H] digoxin, [^{3}H] loperamide and [^{3}H] verapamil are substrates of P-gp and were therefore chosen as markers of the P-gp efflux mechanism (22), to determine the impact of alterations in P-gp expression in AD on brain uptake.

One of the major controversies in AD is related to the status of the BBB paracellular route (and indeed BBB integrity). *In vitro* studies using human brain endothelial cells have shown reduced expression of tight junction proteins and

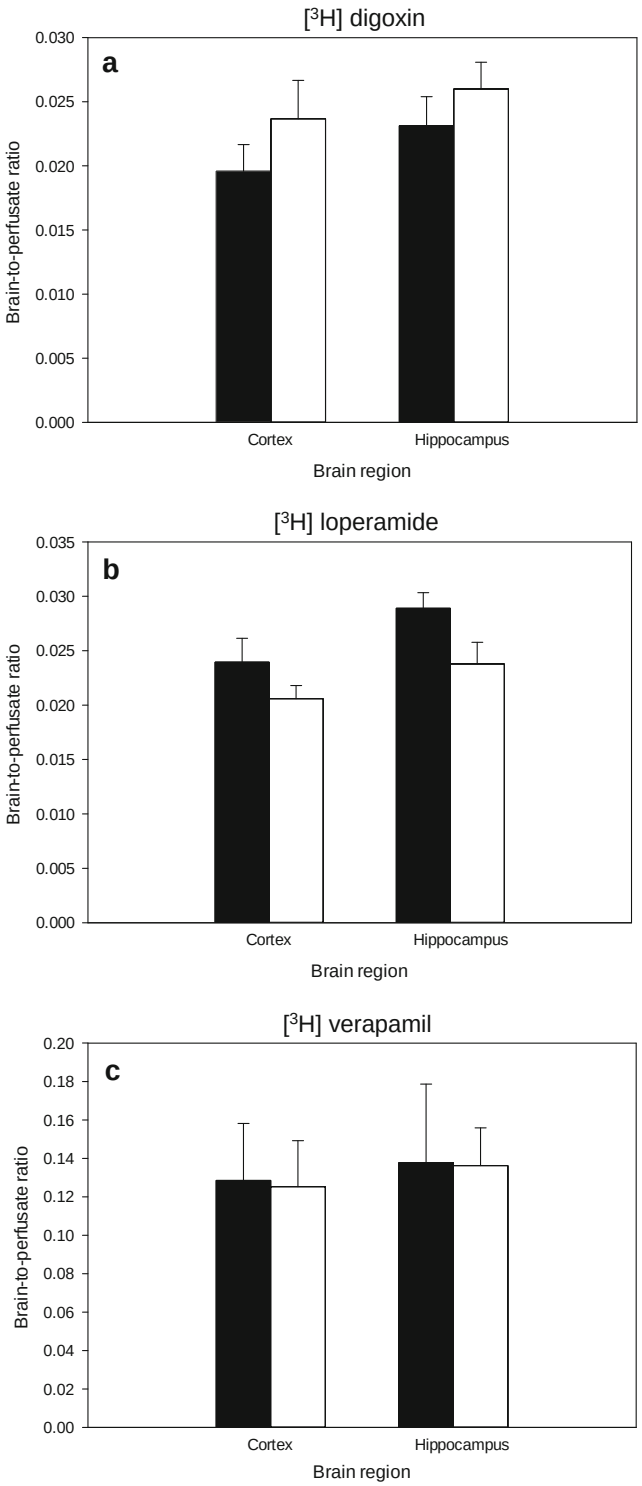

Fig. 4 Brain-to-perfusate ratio of P-gp substrates: (**a**) [^{3}H] digoxin, (**b**) [^{3}H] loperamide and (**c**) [^{3}H] verapamil in cortex and hippocampus following transcardiac perfusion of WT (■) and 3×TG (□) mice. Data are presented as mean ± SEM (n = 6–7 mice).

increased permeability of high molecular weight compounds upon treatment with Aβ (9,34). However the concentrations of Aβ used in these studies (μM) far exceed the pathophysiological concentrations of Aβ observed in AD patients (pM-nM range) (35). Therefore, these studies may lead to results that are not a true representation of the status of the BBB in AD mice and patients. *In vivo* studies using animal models of AD (expressing human APP and/or presenilin transgenes) have depicted increased BBB permeability (with uptake of high molecular weight endogenous or exogenously administered proteins) (14,16). In contrast, in another mouse model of AD, reduced hippocampal and cortical BBB permeability of sucrose and inulin was found, which argues against a massive increase in BBB permeability in AD (17). In addition, clinical studies (using neuroimaging approaches) have suggested no obvious alteration to the functional integrity of the BBB in AD patients (36,37). Thus it can be seen that the integrity of the BBB in AD and its effect on the permeability of compounds remains controversial. Our *in vivo* uptake studies did not demonstrate significant differences in the cortical and hippocampal vascular volume between WT and 3×TG mice. The transcardiac perfusion technique employed in this study is capable of detecting alterations to the BBB paracellular route, as we have observed significant increases in [^{14}C] sucrose uptake in the brain when intentionally disrupting the BBB with lipopolysaccharide (29). The results from this current study suggest that the paracellular route is intact in the 3×TG AD mouse model, consistent with previous clinical studies and an additional *in vivo* mouse study (where no difference in the BBB penetration of [^{131}I] albumin was observed in an alternative model of AD) (15,36,37).

For the first time, this study reports an alteration to the BBB transcellular route in AD, as observed with the decreased uptake of [^{3}H] diazepam and [^{3}H] propranolol in AD-affected regions of 3×TG mice. It is interesting to note that such observations were not made in 3×Tg AD mice at a younger age group (12–14 months of age) (data not presented), suggesting age-dependent effects on the brain uptake of passively-diffusing molecules in the 3×Tg AD mice. Given that the brain uptake of diazepam (and likely propranolol) is blood flow dependent (21,24), and there are reports of reduced cerebral blood flow in AD (6), it could be suggested that the reduction in [^{3}H] diazepam and [^{3}H] propranolol uptake in the 3×Tg AD mice could be a result of reduced cerebral blood flow. However, given that we maintained the perfusion flow at a steady rate throughout the perfusion time, this mechanism is unlikely to be contributing to the reduced uptake of the passively-diffusing markers. According to Fickian diffusion theory, a major factor affecting diffusion across a biological membrane is the membrane thickness, and an increase in membrane thickness is expected to result in reduced permeability (31). The basic element of the healthy basement membrane is collagen type IV, along with other molecular constituents such as heparin sulfate proteoglycans and laminin (6). A thickening of the microvascular basement membrane has been observed in post mortem clinical reports

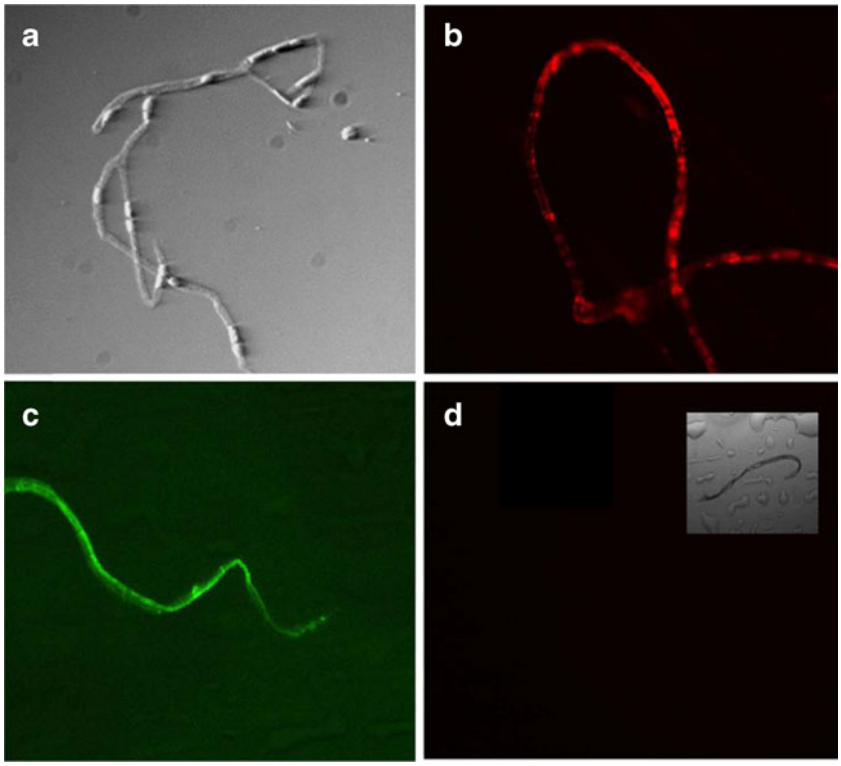

Fig. 5 Characterization of brain microvessels isolated from Swiss outbred mice. (**a**) Phase contrast image of isolated microvessels. Isolated microvessels showing positive staining for P-gp (**b**) and Von-Willebrand factor (**c**) and negative staining for neurons and astrocytes (with inset showing capillary without fluorescence setting) (**d**).

and in an animal model of AD (17,38), which is related to the formation of collagen fibrils forming fiber bundles, with an increased content of collagen type IV in these fibrils (7). We also confirmed in our laboratory (using collagen-IV immunohistochemistry) that there was a significantly thickened basement membrane in the microvessels of 3×TG mice, which is a likely reason for the reduced brain uptake of [^{3}H] diazepam and [^{3}H] propranolol. Furthermore, the thickening of the basement membrane appeared to be in the brain parenchymal direction as a narrowing of the vascular luminal area was not observed. This indeed correlated with our *in vivo* functional studies, as no alteration in the vascular space marker [^{14}C] sucrose was observed between WT and 3×TG mice. The exact reason for the increased content of collagen-IV and subsequent thickening of the basement membrane in AD is not yet fully characterized, however, it does appear to be region-specific with thickening more closely associated with microvessels in AD affected regions than in the microvessels of healthy regions such as the cerebellum (39). Whether this thickening is mediated by the amyloid or tau component of the disease remains unclear. Interestingly though, in a tau-only mouse model, an increase in the area of the capillary wall was observed without any massive distortion in the BBB paracellular permeability, an observation similar to our findings (40). In addition to basement membrane thickening, there have been reports of a reduction in capillary density and abnormalities in microvascular ultrastructure in AD (such as atrophic thin vessels, glomerular loop formations, fragmented vessels and twisted or tortuous vessels) (6,41), which may also potentially impact on the transport of transcellular compounds across the BBB.

In addition to the above explanation, there may be other reasons for the reduced brain uptake of [^{3}H] diazepam and [^{3}H] propranolol in 3×TG AD mice. *In vitro* studies in brain samples obtained from AD and control subjects demonstrates selective changes in the sub units of beta adrenergic and gamma amino butyric acid (GABA) receptors in AD brain with some regions exhibiting lower total concentrations of these receptors in AD patients relative to controls (42–44). This may theoretically reduce the receptor binding of our probe compounds (diazepam and propranolol), thus leading to the observed reduction in their brain uptake in the 3×Tg AD mice. However a small and selective reduction in these receptors in some regions of the brain is unlikely to cause a massive (more than 50%) decrease in the brain uptake of these transcellular marker compounds, as observed in our brain uptake studies. It is possible, however, that both of the above-mentioned hypotheses could contribute, to varying extents, to the observed reduction in the brain uptake of [^{3}H] diazepam and [^{3}H] propranolol.

While passive diffusion appears to be decreased in this mouse model of AD, we were also interested to determine what impact AD had on the transport of P-gp substrates. Clinical studies in non-demented elderly humans have shown an inverse correlation between vascular P-gp expression and Aβ positive plaques, implicating decreased P-gp activity at the BBB in AD (8). Furthermore, P-gp expression in the microvessels of AD mice (harbouring the APP gene) was found

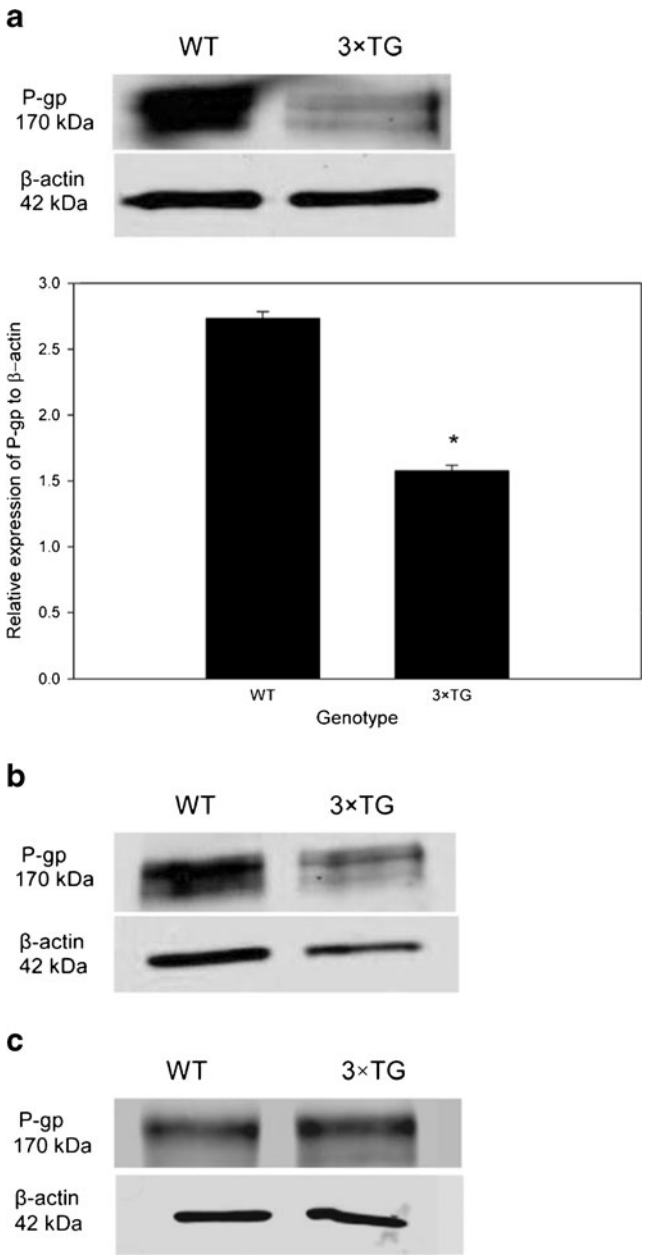

Fig. 6 Western blots depicting P-gp expression in cerebral microvessels isolated from WT and 3×TG mice from three different sub-populations. (**a**) Group 1, where P-gp expression was significantly reduced by 42.4 ± 0.7% ($n = 3$) in 3×TG mice relative to WT (depicted quantitatively in the graph in terms of P-gp expression relative to β-actin in WT and 3×TG mice); (**b**) Group 2, where P-gp expression was reduced by 17% in 3×TG mice compared to WT mice. (**c**) Group 3, where no apparent difference in the expression of P-gp was observed between WT and 3×TG mice. In all three groups, the percentage expression of P-gp was calculated relative to β-actin used as a loading control and analyzed using Image J software. * Indicates a significant ($p < 0.05$) decrease in P-gp expression in 3×TG mice relative to WT mice, using an independent samples *t*-test.

to be reduced to 40% of that observed in WT mice (45). The reduced expression of P-gp observed in AD is hypothesized to lead to an enhanced uptake of P-gp substrates into the brain and undesired neurotoxicity. Therefore it was essential to assess the uptake of P-gp substrates in AD mice. When the P-gp substrates [^{3}H] verapamil, [^{3}H] loperamide and [^{3}H] digoxin were perfused in 3×TG AD mice, we did not observe any significant increase in the uptake of these compounds. To further elucidate our *in vivo* functional results, P-gp expression in the AD mice was measured. Our results clearly demonstrated that P-gp expression was significantly decreased in AD mice, however, there appeared to be one population of AD mice where this reduction was not evident, hinting towards variable alterations in P-gp down-regulation in AD mice. Any expected increase in the brain levels of P-gp substrates (as a result of the decreased P-gp expression) may be counteracted by a thickening of the basement membrane observed in these 3×TG mice, however, further studies would be required to fully elucidate if this indeed is the mechanism responsible for these observations.

It was interesting to observe that, while in two sub-populations of 3×Tg AD mice, the brain microvascular expression of P-gp was significantly reduced, no change in P-gp expression was observed in the third sub-population. This may result from differences in the levels of mediators contributing to P-gp down-regulation within these three sub-populations. While the mechanism by which P-gp expression is lowered in AD is not fully characterized, there are reports that Aβ may directly decrease P-gp expression via inhibition of Wnt/β-catenin signaling (46). Besides Aβ, neuroinflammatory mediators may regulate P-gp expression at the BBB by various mechanisms, leading to both an increase and decrease in P-gp expression (47,48). The reason for our observations of the variable reduction in P-gp expression amongst the three sub-populations of 3×TG mice is not fully known, but it may be related to sub-population specific differences in the levels of the above-mentioned factors that regulate P-gp expression. However, without measuring the levels of Aβ and inflammatory mediators in these three different sub-populations of 3×TG mice, this rationale only remains speculative.

CONCLUSION

In the 3×TG mouse model of AD, the BBB paracellular route of transport appeared unaffected. Rather, our studies imply that the transcellular mechanism of transport across the BBB is reduced in AD, warranting further investigation in the clinical setting with a larger number of lipophilic drug molecules (which traverse the BBB via a transcellular mechanism). These studies are the first to systematically assess the impact of AD on different transport mechanisms across the BBB, suggesting that disposition of therapeutics into the brain may be significantly altered in AD, potentially impacting on clinical outcomes in AD patients.

ACKNOWLEDGMENTS AND DISCLOSURES

The authors would like to acknowledge the JO and JR Wicking Trust, the Mason Foundation, the Helen MacPherson Smith Trust, and ANZ Trustees Program and Medical Research & Technology in Victoria – VCF – George Perry Fund for their financial support. Prof Frank LaFerla (University of California, Irvine) is also acknowledged for the initial supply of the 3×TG AD mouse model.

REFERENCES

1. Selkoe DJ. Alzheimer's disease: genes, proteins, and therapy. Physiol Rev. 2001;81(2):741–66.
2. Alzheimer's Disease Fact Sheet. National Institute on Ageing.; September 2012. Available from: http://www.nia.nih.gov/alzheimers/publication/alzheimers-disease-fact-sheet.
3. Hawkins BT, Davis TP. The blood–brain barrier/neurovascular unit in health and disease. Pharmacol Rev. 2005;57(2):173–85.
4. Nicolazzo JA, Mehta DC. Transport of drugs across the blood–brain barrier in Alzheimer's disease. Ther Deliv. 2010;1(4):595–611.
5. Zlokovic BV. The blood–brain barrier in health and chronic neurodegenerative disorders. Neuron. 2008;57(2):178–201.
6. Farkas E, Luiten PG. Cerebral microvascular pathology in aging and Alzheimer's disease. Prog Neurobiol. 2001;64(6):575–611.
7. Kalaria RN, Pax AB. Increased collagen content of cerebral microvessels in Alzheimer's disease. Brain Res. 1995;705(1–2):349–52.
8. Vogelgesang S, Cascorbi I, Schroeder E, Pahnke J, Kroemer HK, Siegmund W, *et al.* Deposition of Alzheimer's beta-amyloid is inversely correlated with P-glycoprotein expression in the brains of elderly non-demented humans. Pharmacogenetics. 2002;12(7):535–41.
9. Gonzalez-Velasquez FJ, Kotarek JA, Moss MA. Soluble aggregates of the amyloid-β protein selectively stimulate permeability in human brain microvascular endothelial monolayers. J Neurochem. 2008;107(2):466–77.
10. Banks WA. Drug delivery to the brain in Alzheimer's disease: consideration of the blood–brain barrier. Adv Drug Deliv Rev. 2012;64(7):629–39.
11. Deo AK, Theil F-P, Nicolas J-M. Confounding parameters in preclinical assessment of blood–brain barrier permeation: An overview with emphasis on species differences and effect of disease states. Mol Pharmaceutics. 2013;10(5):1581–95.
12. Wada H. Blood–brain barrier permeability of the demented elderly as studied by cerebrospinal fluid-serum albumin ratio. Intern Med. 1998;37(6):509–13.
13. Frölich L, Kornhuber J, Ihl R, Fritze J, Maurer K, Riederer P. Integrity of the blood-CSF barrier in dementia of Alzheimer type: CSF/serum ratios of albumin and IgG. Eur Arch Psychiatry Clin Nuerosci. 1991;240(6):363–6.
14. Ujiie M, Dickstein DL, Carlow DA, Jefferies WA. Blood–brain barrier permeability precedes senile plaque formation in an Alzheimer disease model. Microcirculation. 2003;10(6):463–70.
15. Banks WA, Farr SA, Morley JE. Permeability of the blood–brain barrier to albumin and insulin in the young and aged SAMP8 mouse. J Gerontol A Biol Sci Med Sci. 2000;55(12):601–6.
16. Takechi R, Galloway S, Pallebage-Gamarallage MM, Mamo JC. Chylomicron amyloid-beta in the aetiology of Alzheimer's disease. Atheroscler Suppl. 2008;9(2):19–25.
17. Bourasset F, Ouellet M, Tremblay C, Julien C, Do TM, Oddo S, *et al.* Reduction of the cerebrovascular volume in a transgenic mouse model of Alzheimer's disease. Neuropharmacology. 2009;56(4):808–13.
18. Cheng Z, Zhang J, Liu H, Li Y, Zhao Y, Yang E. Central nervous system penetration for small molecule therapeutic agents does not increase in multiple sclerosis- and Alzheimer's disease-related animal models despite reported blood–brain barrier disruption. Drug Metab Dispos. 2010;38(8):1355–61.
19. Opazo C, Luza S, Villemagne VL, Volitakis I, Rowe C, Barnham KJ, *et al.* Radioiodinated clioquinol as a biomarker for β-amyloid: Zn^{2+} complexes in Alzheimer's disease. Aging Cell. 2006;5(1):69–79.
20. Adlard PA, Cherny RA, Finkelstein DI, Gautier E, Robb E, Cortes M, *et al.* Rapid restoration of cognition in Alzheimer's transgenic mice with 8-hydroxy quinoline analogs is associated with decreased interstitial Aβ. Neuron. 2008;59(1):43–55.
21. Lohmann C, Huwel S, Galla HJ. Predicting blood–brain barrier permeability of drugs:evaluation of different in vitro assays. J Drug Target. 2002;10(4):263–76.
22. Löscher W, Potschka H. Role of drug efflux transporters in the brain for drug disposition and treatment of brain diseases. Prog Neurobiol. 2005;76(1):22–76.
23. Smith QR. Brain perfusion systems for studies of drug uptake and metabolism in the central nervous system. Pharm Biotechnol. 1996;8:285–307.
24. Zhao R, Kalvass J, Pollack G. Assessment of blood–brain barrier permeability using the in situ mouse brain perfusion technique. Pharm Res. 2009;26(7):1657–64.
25. Oddo S, Caccamo A, Shepherd JD, Murphy MP, Golde TE, Kayed R, *et al.* Triple-transgenic model of Alzheimer's disease with plaques and tangles: intracellular Aβ and synaptic dysfunction. Neuron. 2003;39(3):409–21.
26. Mastrangelo MA, Bowers WJ. Detailed immunohistochemical characterization of temporal and spatial progression of Alzheimer's disease-related pathologies in male triple-transgenic mice. BMC Neurosci. 2008;9(81):1–31.
27. Nicolazzo JA, Charman SA, Charman WN. Methods to assess drug permeability across the blood–brain barrier. J Pharm Pharmacol. 2006;58(3):281–93.
28. Banks WA, Morley JE, Lynch JL, Lynch KM, Mooradian AD. Insulin detemir is not transported across the blood–brain barrier. Peptides. 2010;31(12):2284–8.
29. Jin L, Li J, Nation RL, Nicolazzo JA. Impact of P-glycoprotein inhibition and lipopolysaccharide administration on blood–brain barrier transport of colistin in mice. Antimicrob Agents Chemother. 2011;55(2):502–7.
30. Braak H, Braak E. Frequency of stages of Alzheimer-related lesions in different age categories. Neurobiol Aging. 1997;18(4):351–7.
31. Zwolinski BJ, Eyring H, Reese CE. Diffusion and membrane permeability. J Phys Chem. 1948;53(9):1426–53.
32. Yousif S, Marie-Claire C, Roux F, Scherrmann J-M, Declèves X. Expression of drug transporters at the blood–brain barrier using an optimized isolated rat brain microvessel strategy. Brain Res. 2007;1134:1–11.
33. Cattelotte J, Andre P, Ouellet M, Bourasset F, Scherrmann JM, Cisternino S. In situ mouse carotid perfusion model: glucose and cholesterol transport in the eye and brain. J Cereb Blood Flow Metab. 2008;28:1449–59.
34. Tai LM, Holloway KA, Male DK, Loughlin AJ, Romero IA. Amyloid-β-induced occludin down-regulation and increased permeability in human brain endothelial cells is mediated by MAPK activation. J Cell Mol Med. 2010;14(5):1101–12.
35. Mehta PD, Pirttila T, Patrick BA, Barshatzky M, Mehta SP. Amyloid β protein 1–40 and 1–42 levels in matched cerebrospinal fluid and plasma from patients with Alzheimer disease. Neurosci Lett. 2001;304(1–2):102–6.
36. Caserta MT, Caccioppo D, Lapin GD, Ragin A, Groothuis DR. Blood–brain barrier integrity in Alzheimer's disease patients and

elderly control subjects. J Neuropsychiatry Clin Neurosci. 1998;10(1):78–84.
37. Starr JM, Farrall AJ, Armitage P, McGurn B, Wardlaw J. Blood–brain barrier permeability in Alzheimer's disease: a case–control MRI study. Psychiatry Res. 2009;171(3):232–41.
38. Claudio L. Ultrastructural features of the blood–brain barrier in biopsy tissue from Alzheimer's disease patients. Acta Neuropathol. 1995;91(1):6–14.
39. Zarow C, Barron E, Chui HC, Perlmutter LS. Vascular basement membrane pathology and Alzheimer's disease. Ann N Y Acad Sci. 1997;826(1):147–59.
40. Jaworski T, Lechat B, Demedts D, Gielis L, Devijver H, Borghgraef P, *et al.* Dendritic degeneration, neurovascular defects, and inflammation precede neuronal loss in a mouse model for tau-mediated neurodegeneration. Am J Pathol. 2011;179(4):2001–15.
41. Buee L, Hof P, Delacourte A. Brain microvascular changes in Alzheimer's disease and other dementias. Ann N Y Acad Sci. 1997;826(1):7–24.
42. Shimohama S, Taniguchi T, Fujiwara M, Kameyama M. Changes in β-adrenergic receptor subtypes in Alzheimer-type dementia. J Neurochem. 1987;48(4):1215–21.
43. Kalaria RN, Andorn AC, Tabaton M, Whitehouse PJ, Harik SI, Unnerstall JR. Adrenergic receptors in aging and Alzheimer's disease: increased β_2-receptors in prefrontal cortex and hippocampus. J Neurochem. 1989;53(6):1772–81.
44. Limon A, Reyes-Ruiz JM, Miledi R. Loss of functional $GABA_A$ receptors in the Alzheimer diseased brain. Proc Natl Acad Sci U S A. 2012;109(25):10071–6.
45. Hartz AM, Miller DS, Bauer B. Restoring blood–brain barrier P-glycoprotein reduces brain amyloid-β in a mouse model of Alzheimer's disease. Mol Pharmacol. 2010;77(5):715–23.
46. Kania KD, Wijesuriya HC, Hladky SB, Barrand MA. Beta amyloid effects on expression of multidrug efflux transporters in brain endothelial cells. Brain Res. 2011;1418:1–11.
47. Bauer B, Hartz AMS, Miller DS. Tumor necrosis factor α and endothelin-1 increase P-glycoprotein expression and transport activity at the blood–brain barrier. Mol Pharmacol. 2007;71(3):667–75.
48. Salkeni M, Lynch J, Otamis-Price T, Banks W. Lipopolysaccharide impairs blood–brain barrier P-glycoprotein function in mice through prostaglandin- and nitric oxide-independent pathways. J Neuroimmune Pharmacol. 2009;4(2):276–82.